

# Differentiable Subset Pruning of Transformer Heads

Jiaoda Li<sup>♣</sup> Ryan Cotterell<sup>♣♠</sup> Mrinmaya Sachan<sup>♣</sup>

<sup>♣</sup>ETH Zürich, Switzerland <sup>♠</sup>University of Cambridge, UK

{jiaoda.li,ryan.cotterell,mrinmaya.sachan}@inf.ethz.ch

## Abstract

Multi-head attention, a collection of several attention mechanisms that independently attend to different parts of the input, is the key ingredient in the Transformer. Recent work has shown, however, that a large proportion of the heads in a Transformer’s multi-head attention mechanism can be safely pruned away without significantly harming the performance of the model; such pruning leads to models that are noticeably smaller and faster in practice. Our work introduces a new head pruning technique that we term differentiable subset pruning. Intuitively, our method learns per-head importance variables and then enforces a user-specified hard constraint on the number of unpruned heads. The importance variables are learned via stochastic gradient descent. We conduct experiments on natural language inference and machine translation; we show that differentiable subset pruning performs comparably or better than previous works while offering precise control of the sparsity level.<sup>1</sup>

## 1 Introduction

The Transformer (Vaswani et al., 2017) has become one of the most popular neural architectures used in NLP. Adaptations of the Transformer have been applied to nearly every popular NLP task, for example, parsing (Zhou and Zhao, 2019), machine translation (Ng et al., 2019), question answering (Yang et al., 2019) inter alia. Transformers also form the backbone of state-of-the-art pre-trained language models, for example, BERT (Devlin et al., 2019), GPT-2 (Radford et al., 2019), and GPT-3 (Brown et al., 2020), that have further boosted performance on various data-driven NLP problems. The key ingredient in the Transformer architecture is the multi-head attention mechanism, which is an assembly of multiple attention functions (Bahdanau et al., 2015) applied in parallel. In

practice, each attention head works independently, which allows the heads to capture different kinds of linguistic phenomena (Clark et al., 2019; Goldberg, 2019; Ettinger, 2020; Jawahar et al., 2019). A natural question arises in this context: How many heads does a transformer need?

Michel et al. (2019) offer the insight that *a large portion of the Transformer’s heads can be pruned without significantly degrading the test accuracy on the desired task*. The experimental evidence behind their claim is a simple greedy procedure that sequentially removes heads. This suggests that a better pruner could reveal that a much larger portion of the heads can be safely removed. To provide a more robust answer to Michel et al.’s question, we build a high-performance pruner and show that their approach itself significantly underestimates the number of Transformer heads that can be pruned away.

From a bird’s eye view, our paper contributes the proposal that Transformer head pruning is best viewed as a **subset selection** problem. Subset selection is common across many areas of NLP, from extractive summarization (Gillenwater et al., 2012) to vowel typology (Cotterell and Eisner, 2017). In the case of head pruning, the concrete idea is that the user specifies a number of heads  $K$  that they would like their Transformer to have depending on their budgetary and other constraints, and then the pruner enforces this constraint. Methodologically, we present a differentiable subset pruner (Figure 1) that makes use of Gumbel machinery; specifically, the Gumbel top- $K$  procedure of Vieira (2014). This construction allows us to relax our pruner into a differentiable sampling routine that qualitatively resembles a discrete analogue of dropout (Srivastava et al., 2014; Gal and Ghahramani, 2016).

Empirically, we perform experiments on two common NLP tasks: natural language inference (MNLI; Williams et al., 2018) and machine translation (IWSLT2014; Cettolo et al., 2014). We show that our differentiable subset pruning scheme

<sup>1</sup>Our code is available here: <https://github.com/rycolab/differentiable-subset-pruning>.

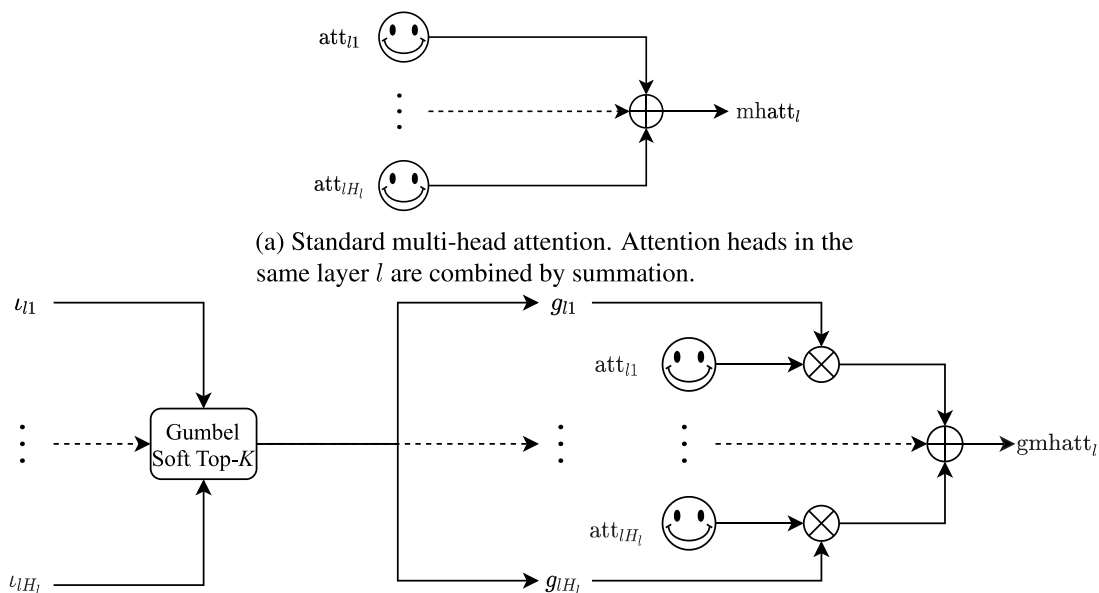


Figure 1: Illustration of gated multi-head attention compared with standard multi-head attention.

outperforms two recently proposed Transformer head pruners—Michel et al. (2019) and Voita et al. (2019)—on both tasks in terms of sparsity–performance trade-off. Our method recovers a pruned Transformer that has  $\approx 80\%$  accuracy on MNLI and  $\approx 30$  BLEU score on IWSLT when more than 90% of the heads are removed, which brings about  $\approx 33\%$  inference speedup and  $\approx 24\%$  model size shrinkage.<sup>2</sup>

Our experiments also suggest several broader conclusions about pruning Transformers. In this paper, we taxonomize existing pruning methods into two pruning paradigms: pipelined pruning and joint pruning. **Pipelined pruning** consists of two stages: (i) training or fine-tuning an over-parameterized model on the target task and (ii) pruning the model after training. A number of techniques fall into this category (LeCun et al., 1990; Hassibi et al., 1994; Han et al., 2016; Molchanov et al., 2017b). In contrast, **joint pruning** blends the pruning objective into the training objective by training or fine-tuning the over-parameterized model with a sparsity-enforcing regularizer, sometimes followed up by a trivial post-processing step to arrive at a final sparse model. Kingma et al. (2015) and Louizos et al. (2018) are examples of

<sup>2</sup>See § 5.4.

this kind of pruning. We show that pipelined head pruning schemes, such as that of Michel et al., underperform compared to joint head pruning schemes, such as that of Voita et al. (2019). Our differentiable subset pruner can be adapted to both paradigms and it outperforms prior work in both, especially in high sparsity regions.

## 2 Background: Multi-head Attention

In this section, we provide a detailed overview of multi-head attention (Vaswani et al., 2017) in order to develop the specific technical vocabulary to discuss our approaches for head pruning. We omit details about other parts of the Transformer and refer the reader back to the original work of Vaswani et al. (2017). First, let  $\mathbf{z} = z_1, \dots, z_T$  be a sequence of  $T$  real vectors where  $z_t \in \mathbb{R}^d$ , and let  $q \in \mathbb{R}^d$  be a query vector. An **attention mechanism** is defined as

$$\text{att}(\mathbf{z}, q) = W_o \sum_{t=1}^T \alpha_t(q) W_v z_t \quad (1)$$

where

$$\alpha_t(q) = \text{softmax} \left( \frac{q^\top W_q^\top W_k z_t}{\sqrt{d}} \right)_t \quad (2)$$

The projection matrices  $W_o, W_v, W_q, W_k \in \mathbb{R}^{d \times d}$  are learnable parameters. In self-attention, query  $q$  comes from the same sequence  $\mathbf{z}$ .

A Transformer is composed of  $L$  identical layers. In layer  $1 \leq l \leq L$ ,  $H_l$  different attention mechanisms are applied in parallel; importantly, it is this parallelism that has led to the rise of the Transformer—it is a more efficient architecture in practice so it can be trained on more data. Each individual attention mechanism is referred to as a **head**; thus, **multi-head attention** is the simultaneous application of multiple attention heads in a single architecture. In Vaswani et al. (2017), the multiple heads are combined through summation:

$$\text{mhatt}_l(\mathbf{z}, q) = \sum_{h=1}^{H_l} \text{att}_{lh}(\mathbf{z}, q) \quad (3)$$

where  $\text{att}_{lh}$  is the  $h^{\text{th}}$  attention head in the  $l^{\text{th}}$  layer. We also introduce a **gate variable**  $g_{lh}$  that takes values in the interval  $[0, 1]$ :

$$\text{gmhatt}_l(\mathbf{z}, q) = \sum_{h=1}^{H_l} g_{lh} \cdot \text{att}_{lh}(\mathbf{z}, q) \quad (4)$$

Inserting  $g_{lh}$  into the multi-head attention enables our pruning approach: setting the gate variable to  $g_{lh} = 0$  means the head  $\text{att}_{lh}$  is pruned away.

In the following sections, for the sake of notational simplicity, we ignore the layer structure of heads and label heads with a single index  $h \in \{1, \dots, H\}$ , where  $H = \sum_{l=1}^L H_l$  is the total number of heads in the unpruned model.

### 3 Differentiable Subset Pruning

In this section, we propose a new head pruning technique that we term **differentiable subset pruning**. The key insight behind our approach is that head pruning can be viewed as subset selection. Concretely, our goal is to find a subset of  $K$  heads (where  $K$  is a user-specified positive integer) that still allows the model to achieve high performance. Many neural network pruners, for example, Voita et al.’s (2019) proposed head pruning technique, make it notably difficult to pre-specify the number of pruned heads  $K^3$ . To make our subset pruner differentiable, we apply the Gumbel–softmax trick (Maddison et al., 2017)

<sup>3</sup>Later discussed in § 5.2.

and its extension to subset selection (Vieira, 2014; Xie and Ermon, 2019). This gives us a pruning scheme that always returns the specified number of heads and can be applied in a pipelined or a joint setting. In both cases, the differentiability is necessary to learn the head weights.

#### 3.1 Background: Gumbel-(soft)max

Let  $\mathcal{H} = \{1, \dots, H\}$  be the set of Transformer heads in a given architecture. Our goal is to return a subset of head  $\mathcal{J} \subseteq \mathcal{H}$  where  $|\mathcal{J}| = K$  for any user-specified value of  $K$ . We use the notation  $\iota_h > 0$  to denote a head **importance score** of the specific head  $h$ . The head importance score intuitively corresponds to how much we would like to have the head  $h$  in the subset of heads  $\mathcal{J}$ .

We start our exposition by reviewing the Gumbel trick in the context of selecting a single head ( $K = 1$ ) and then move onto discussing its extension to subset selection. Given the head importance scores  $\iota_h$ , suppose we would like to sample a subset  $\mathcal{J}$  of size 1 according to the following distribution

$$p(\mathcal{J} = \{h\}) = \frac{\iota_h}{Z} \propto \iota_h \quad (5)$$

where  $Z = \sum_{h=1}^H \iota_h$  is the normalization constant. The simplest way to achieve this is to use standard categorical sampling. However, as has been noted by Maddison et al. (2014), categorical sampling is not differentiable. Luckily, there is a two-step process to massage categorical sampling into a differentiable sampling procedure: (1) reparameterize the categorical using Gumbels and (2) soften the argmax into a softmax.

##### 3.1.1 Step 1: Reparameterization

We can reparameterize categorical sampling using the Gumbel-max trick (Gumbel, 1954) to first separate the sampling from the parameter that we wish to differentiate with respect to. The idea of the Gumbel max trick is that categorical sampling can be viewed as a perturb-and-max method. If we first perturb the logits  $\log(\iota_h)$  with Gumbel noise  $n_h \sim \text{Gumbel}(0, 1)$  such that  $r_h = \log(\iota_h) + n_h$ , then sampling from a categorical is equivalent to taking an argmax:

$$h^* = \underset{h \in \mathcal{H}}{\text{argmax}} r_h \quad (6)$$

Were argmax differentiable, we would be done; unfortunately it is not.

### 3.1.2 Step 2: Relaxing the argmax

Now to construct a fully differentiable procedure, we replace the argmax with a softmax. The intuition here is that the output of argmax may be viewed as an one-hot vector with the one corresponding to the index of the argmax.<sup>4</sup> The insight, then, is to relax the one-hot vector output by the argmax into a softmax as follows:

$$g_h = \frac{\exp(r_h)}{\sum_{h'=1}^H \exp(r_{h'})} \quad (7)$$

This technique is called the Gumbel-softmax trick (Jang et al., 2017), and the resulting distribution is known as the Concrete distribution (Maddison et al., 2017).<sup>5</sup> It is often desirable to add an additional annealing parameter  $\tau > 0$  to the Gumbel-softmax:

$$g_h = \frac{\exp(r_h/\tau)}{\sum_{h'=1}^H \exp(r_{h'}/\tau)} \quad (8)$$

As the temperature tends to zero, that is,  $\tau \rightarrow 0$ , the softmax turns into the argmax. Thus, through the tunable  $\tau$ , we can arbitrarily approximate the argmax as a differentiable function.

## 3.2 Differentiable Subset Selection

The Gumbel trick can be generalized to cases where we wish to sample an entire set of heads. This is called the Gumbel-top- $K$  trick. The idea is that, rather than simply taking the max, we sort and take the top- $K$  largest perturbed logits (Yellott, 1977; Vieira, 2014; Kool et al., 2019). One way to think of the algorithm is that we are repeating the Gumbel trick  $K$  times until we have the desired number of heads. Following the exposition in § 3.1, we divide our discussion into two sections.

### 3.2.1 Step 1: Reparameterization

Similar to the top-1 case, we start by sampling the first head using the perturb-and-max strategy:

$$h_1^* = \operatorname{argmax}_{h \in \mathcal{H}} r_h \quad (9)$$

<sup>4</sup>More precisely, argmax returns a set. In our terminology, it would return a multi-hot vector. We ignore this case in our exposition for simplicity.

<sup>5</sup>Using the Gumbel-softmax results in a biased estimate of the gradient. Subsequent work removed this bias (Tucker et al., 2017).

Then we remove  $h_1^*$  from the pool of heads under consideration and repeat the same procedure:

$$h_2^* = \operatorname{argmax}_{h \in \mathcal{H} \setminus \{h_1^*\}} r_h \quad (10)$$

⋮

$$h_K^* = \operatorname{argmax}_{h \in \mathcal{H} \setminus \{h_1^*, \dots, h_{K-1}^*\}} r_h \quad (11)$$

The probability of sampling these heads *in this order* is given by the following expression:

$$p(h_1^*, \dots, h_K^*) = \frac{\iota_{h_1^*}}{Z} \cdots \frac{\iota_{h_K^*}}{Z - \sum_{k=1}^{K-1} \iota_{h_k^*}} \quad (12)$$

Thus, the probability of a set  $\mathcal{J}$  is given by

$$\begin{aligned} p(\mathcal{J} = \{h_1^*, \dots, h_K^*\}) & \quad (13) \\ &= \sum_{\pi \in \mathbb{S}_K} p(h_{\pi_1}^*, \dots, h_{\pi_K}^*) \end{aligned}$$

where  $\mathbb{S}_K$  is the set of all permutations of  $K$  items. This is hard to compute as it involves a sum over permutations. For a detailed discussion on computing (13), we refer the reader to the discussion in Vieira (2021a) and Vieira (2021b). Ultimately, however, computing the exact probability of a subset of heads  $\mathcal{J}$  is unnecessary for this approach.

As an aside, we note that this procedure is equivalent to a differentiable version of the classical reservoir sampling algorithm (Vitter, 1985).

### 3.2.2 Step 2: Relaxing the argmax

The Gumbel-top- $K$  trick can be relaxed similarly to the top-1 case. This was first shown in detail by Xie and Ermon (2019). Here, we provide a detailed overview of the algorithm by analogy to the top-1 case. Similarly, the output of Gumbel-top- $K$  can be viewed as a  $K$ -hot vector, which is the sum of the  $K$  one-hot vectors produced in (9)–(11). As before, we begin by relaxing the one-hot vector of the first head:

$$g_h^{(1)} = \frac{\exp(r_h^{(1)}/\tau)}{\sum_{h'=1}^H \exp(r_{h'}^{(1)}/\tau)} \quad (14)$$

This is a straight-forward analogue of the argmax relaxation discussion in § 3.1.2. Next, we continue

relaxing the successive argmaxes with successive softmaxes (Plötz and Roth, 2018) as follows:

$$g_h^{(2)} = \frac{\exp(r_h^{(2)}/\tau)}{\sum_{h'=1}^H \exp(r_{h'}^{(2)}/\tau)} \quad (15)$$

$$\vdots$$

$$g_h^{(K)} = \frac{\exp(r_h^{(K)}/\tau)}{\sum_{h'=1}^H \exp(r_{h'}^{(K)}/\tau)} \quad (16)$$

where the  $r_h^{(k)}$  are defined recursively

$$r_h^{(1)} = r_h \quad (17)$$

$$r_h^{(k+1)} = r_h^{(k)} + \log(1 - g_h^{(k)}) \quad (18)$$

Xie and Ermon (2019) argue that the above recursion corresponds to a reasonable relaxation of the Gumbel-top- $K$  trick presented in § 3.2.1. To understand the motivation behind the recursion in (17), note that if  $g_h^{(k)} = 1$ , which would happen if the head has been sampled (i.e., no relaxation), then that head would not be selected again as we have  $r_h^{(k+1)} = -\infty$ . As the scheme is a relaxation of hard sampling, we will not have  $g_h^{(k)} = 1$  as long as  $r_h^{(k)}$  is finite and  $\tau > 0$ . Thus, the procedure corresponds to something akin to a soft sampling.

Finally, we sum over all the relaxed one-hot vectors  $g_h^{(k)}$  in (14)–(16) to arrive at our softened  $K$ -hot gate:

$$g_h = \sum_{k=1}^K g_h^{(k)} \quad (19)$$

It is (19) that we finally plug into the gated attention mechanism presented in (2).

### 3.3 Training the Subset Pruner

The differentiable subset pruning approach can be applied in either a pipelined or a joint pruning setting. (Please refer back to the last paragraph of § 1 for a discussion of the two different settings.) Our approach is parameterized identically in both settings, however. Specifically, we define head importance score as follows:

$$\iota_h = \exp(w_h) \quad (20)$$

where  $w_h$  is the  $h^{\text{th}}$  component of a vector of real-valued head weights  $\mathbf{w} \in \mathbb{R}^H$ . In our setting, the distinction between pipelined pruning and joint

pruning is relatively trivial. In the pipelined setting, we learn the head importance weights  $\mathbf{w}$  for a model that has been trained on the task and leave the model parameters untouched. On the other hand, in the joint setting, we simultaneously learn the head importance weights and the model parameters. In this regard, our differentiable subset pruner much more closely resembles Voita et al.’s (2019) method in that we *learn* head-specific importance weights. On the other hand, Michel et al.’s (2019) method makes use of an unlearned gradient-based importance measure. In contrast to Voita et al., however, our differentiable subset pruner ensures that it returns a specific pre-specified number of heads.

## 4 Experiments

### 4.1 Model and Data

We investigate two Transformer-based models in the empirical portion of the paper.

**BERT.** BERT (Bidirectional Encoder Representations from Transformers; Devlin et al., 2019) is essentially a Transformer encoder. Since there is no decoder part, BERT only has self-attention. We focus on the `base-uncased` model with 12 layers and 12 heads in each layer (144 heads in total). We use the implementation of Hugging Face (Wolf et al., 2020). The model is pre-trained on large text corpora using masked language modeling (MLM) and next sentence prediction (NSP). We fine-tune BERT on the Multi-Genre Natural Language Inference (MNLI; Williams et al., 2018) corpus. The hyper-parameters are tuned on the “matched” validation set, and accuracy is reported on the “mismatched” validation set.

**Enc-Dec.** We implement a Transformer-based encoder-decoder model with 6 encoder layers, 6 decoder layers and 6 heads in each layer (72 heads in total). The model has three types of attention heads: encoder self-attention, decoder self-attention, and encoder-decoder cross attention. We use the `fairseq` toolkit (Ott et al., 2019) for our implementation. We train the model on the International Workshop on Spoken Language Translation (IWSLT2014; Cettolo et al., 2014) German-to-English dataset. The hyper-parameters are tuned on the validation set, and 4-gram BLEU scores computed with `multi-bleu.perl` (Koehn et al., 2007) are reported on the held-out

test set. We use beam search with a beam size set to 5 for decoding.

## 4.2 Baselines

We compare our approach to pruners in both the pipelined and the joint paradigms. We refer to the pipelined version of our differentiable subset pruning as **pipelined DSP** and to the joint version as **joint DSP**. Our specific points of comparison are listed below.

### 4.2.1 Michel et al.

Michel et al. follow the pipelined pruning paradigm. Concretely, given a dataset  $\mathcal{D} = \{(\mathbf{y}_m, \mathbf{x}_m)\}_{m=1}^M$ , the importance of a head is estimated with a gradient-based proxy score (Molchanov et al., 2017b):

$$\iota_h = \frac{1}{M} \sum_{m=1}^M \left| \frac{\partial \mathcal{L}(\mathbf{y}_m, \mathbf{x}_m)}{\partial g_h} \right| \geq 0 \quad (21)$$

where  $\mathcal{L}$  is the task-specific loss function. Then, all the heads in the model are sorted accordingly and removed one by one in a greedy fashion. The importance scores are re-computed every time a certain number of heads are removed.

### 4.2.2 Voita et al.

In the fashion of joint pruning, Voita et al. apply a stochastic approximation to  $L_0$  regularization (Louizos et al., 2018) to the gates to encourage the model to prune less important heads. The gate variables are sampled from a binary Hard Concrete distribution (Louizos et al., 2018) independently, parameterized by  $\phi_h$ . The  $L_0$  norm was relaxed into the sum of probability mass of gates being non-zero:

$$L_C(\phi) = \sum_{h=1}^H (1 - P(g_h = 0 | \phi_h)) \quad (22)$$

which was then added to the task-specific loss  $\mathcal{L}$ :

$$\mathcal{R}(\theta, \phi) = \mathcal{L}(\theta, \phi) + \lambda L_C(\phi) \quad (23)$$

where  $\theta$  are the parameters of the original model, and  $\lambda$  is the weighting coefficient for the regularization, which we can use to indirectly control the number of heads to be kept.

### 4.2.3 Straight-Through Estimator (STE)

In this baseline, the Gumbel soft top- $K$  in joint DSP is replaced with hard top- $K$ , while the hard

top- $K$  function is back-propagated through as if it had been the identity function, which is also termed as straight-through estimator (Bengio et al., 2013).

### 4.2.4 Unpruned Model

The model is trained or fine-tuned without any sparsity-enforcing regularizer and no post-hoc pruning procedure is performed. We take this comparison to be an upper bound on the performance of any pruning technique.

## 4.3 Experimental Setup

**Pipelined Pruning.** For the two pipelined pruning schemes, the model is trained or fine-tuned on the target task (3 epochs for BERT and 60 epochs for Enc-Dec) before being pruned. We learn the head importance weights for pipelined DSP for one additional epoch in order to have an apples-to-apples comparison with Michel et al. in terms of compute (number of gradients computed).

**Joint Pruning.** The model is trained or fine-tuned for the same number of epochs as pipelined pruning while sparsity-enforcing regularization is applied. We found it hard to tune the weighting coefficient  $\lambda$  for Voita et al. to reach the desired sparsity (see § 5.2 and Figure 3). For the ease of comparison with other approaches, we adjust the number of unpruned heads to the targeted number by re-including heads with the highest gate values from the discarded ones, or excluding those with the smallest gate values in the kept ones. We make sure the adjustments are as small as possible.

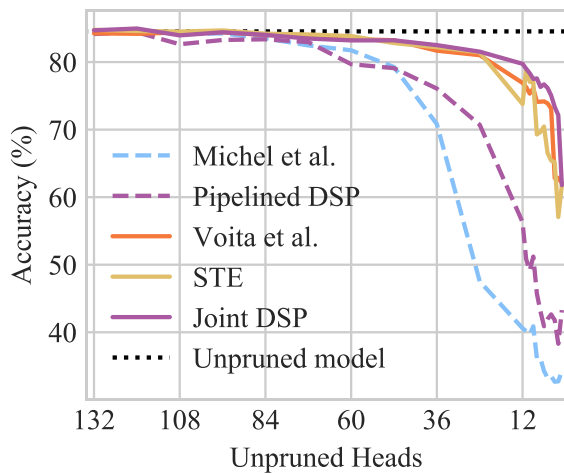
**Annealing Schedule.** In our experiments, we choose a simple annealing schedule for DSP where the temperature  $\tau$  cools down in a log-linear scale within a predefined number of steps  $N_{\text{cooldown}}$  from an initial temperature  $\tau_{\text{ini}}$  and then stays at the final temperature  $\tau_{\text{end}}$  for the rest of the training steps:

$$\log \tau = \log \tau_{\text{ini}} - \min \left\{ \frac{n}{N_{\text{cooldown}}}, 1 \right\} \cdot (\log \tau_{\text{ini}} - \log \tau_{\text{end}}) \quad (24)$$

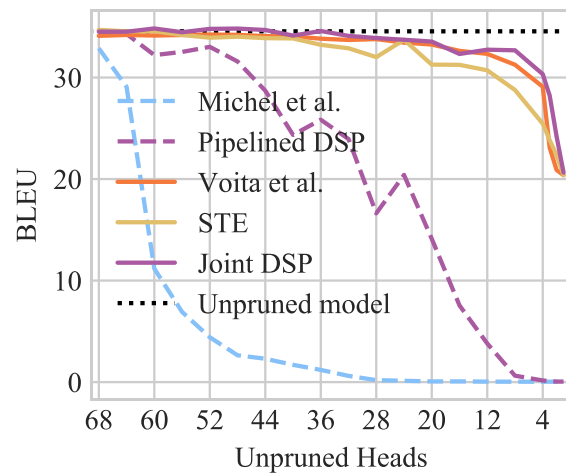
where  $n$  is the number of training steps that has been run. We report the set of hyperparameters used in our experiments in Appendix A.

## 4.4 Results

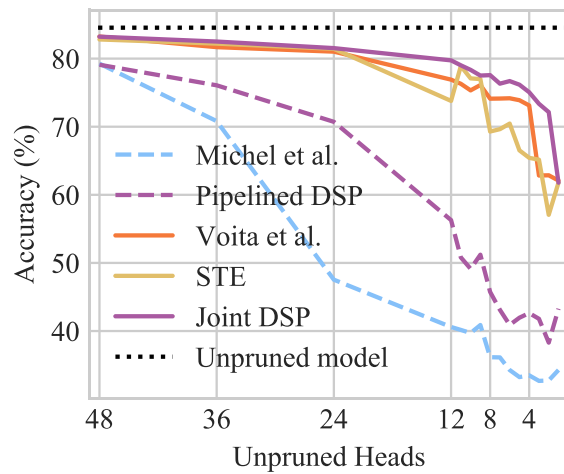
The test performance under various sparsity levels obtained by multiple pruning methods are



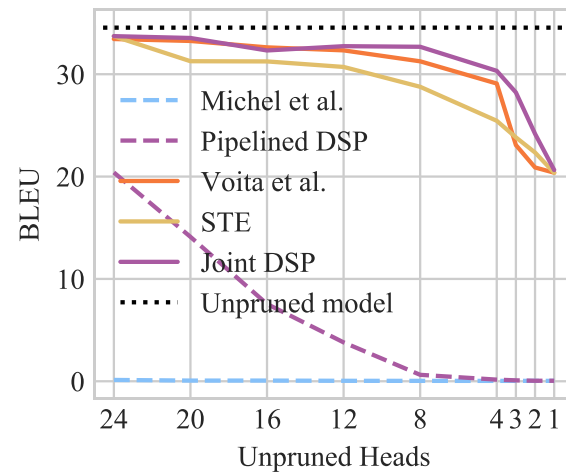
(a) Accuracy on the MNLI-mismatched validation set as a function of number of unpruned heads in BERT.



(b) BLEU score on IWSLT test set as a function of number of unpruned heads in Enc-Dec.



(c) We zoom in on the portion of Fig. 2a where few heads remain unpruned.



(d) We zoom in on the portion of Fig. 2b where few heads remain unpruned.

Figure 2: A comparison of various pruning methods.

presented in Figure 2a, Figure 2b, and Appendix C. We also zoom in to results when more than two-thirds of the heads are pruned in Figure 2c and Figure 2d, where the differences between the various methods are most evident.

## 5 Discussion

### 5.1 Pipelined Pruning

We first compare the two pipelined pruning methods: Michel et al. (2019) and pipelined DSP. As shown in Figure 2, pipelined DSP outperforms Michel et al. by a large margin. For example, on the MNLI task, when there are 24 heads left in the model, pipelined DSP keeps an accuracy above 70%, but Michel et al. drops below 50%. On the

IWSLT dataset, when only 24 heads are left unpruned, the Enc-Dec pruned with Michel et al. cannot produce meaningful outputs ( $\approx 0$  BLEU score), while pipelined DSP achieves higher than 20 BLEU. The results indicate that the learned head importance scores are more useful for pruning than those computed with gradient-based measures.

### 5.2 Joint Pruning

We then compare the three joint pruning methods: Voita et al. (2019), STE, and joint DSP. Impressively, joint DSP is able to prune up to 91.6% (12 heads left) and 94.4% (4 heads left) of heads in BERT and the Enc-Dec, respectively, without causing much degradation in test performance

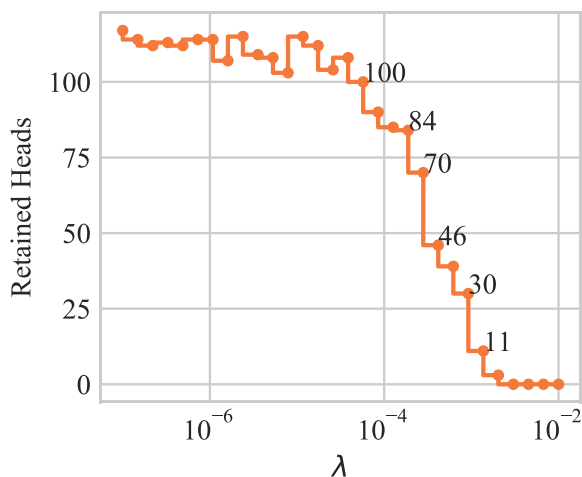


Figure 3: Number of unpruned heads as a function of  $L_0$  regularization coefficient  $\lambda$  for Voita et al.

(5.5% drop in accuracy for MNLI and 4.22 drop in BLEU score for IWSLT). Voita et al. and STE are neck and neck with joint DSP when the model is lightly pruned, but joint DSP gains the upper hand when less than  $\frac{1}{6}$  of the heads are left unpruned.

In addition, with Voita et al.’s method, it is much harder to enforce a hard constraint on the number of unpruned heads. This difficulty is intrinsic to their method as Voita et al.’s method relies on the regularization coefficient  $\lambda$  to indirectly control the sparsity. In practice, our experiments indicate that  $\lambda$  is hard to tune and there are certain levels of sparsity that cannot be reached. The difficulty in tuning  $\lambda$  is shown in Figure 3; we see that the number of unpruned heads does not decrease monotonically as  $\lambda$  increases; on the contrary, it often fluctuates. There also appears to be an upper bound (117) on the number of heads that can be kept no matter how small  $\lambda$  is. More importantly, a small increase in  $\lambda$  can sometimes drastically reduce the number of heads. For instance, when  $\lambda$  is increased from 0.0009 to 0.0014, the number of heads reduced quickly from 30 to 11. Therefore, we conclude that Voita et al.’s method is inadequate if the user requires a pre-specified number of Transformer heads. In contrast, DSP (as well as STE), our proposal, enables us to directly specify the number of heads we want to keep in accordance with our computation budget.

### 5.3 Pipelined Pruning vs Joint Pruning

Lastly, we offer a philosophical comparison of the two pruning paradigms. It is clear from Figure 2

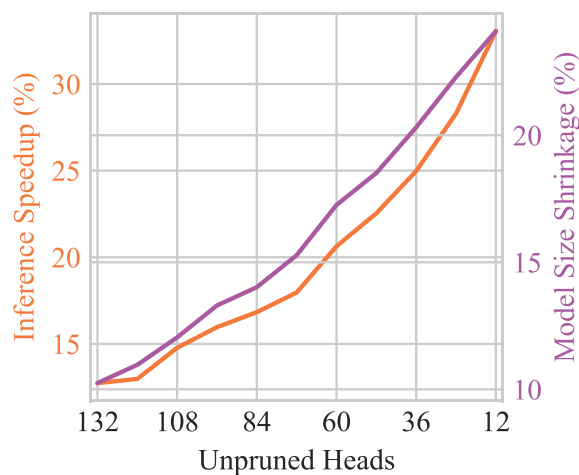


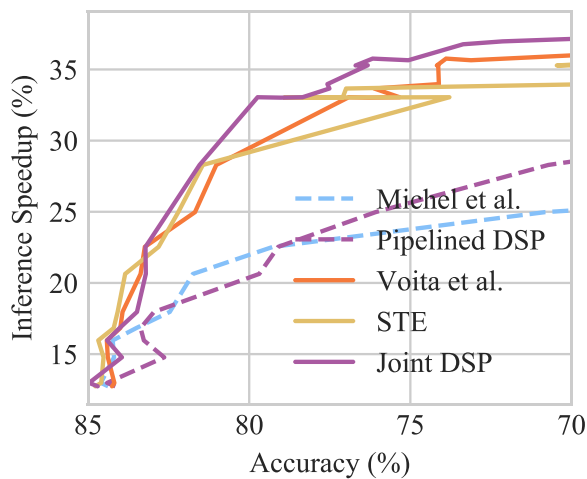
Figure 4: Inference speedup (%) and model size shrinkage (%) of pruned BERT model on the MNLI-mismatched validation set as a function of remaining heads.

that the joint pruning methods are superior to pipelined pruning methods for both tasks, as models sparsified with the joint pruning schemes (joint DSP, STE and Voita et al.) perform better than those pruned with pipelined schemes (pipelined DSP and Michel et al.) under almost every sparsity level. This suggests that joint training is more effective in finding sparse subnetworks than pipelined pruning. Moreover, joint pruning is also more computationally efficient. In addition to the same number of epochs required by both paradigms for training/fine-tuning, pipelined pruning requires us to learn or estimate gradient-based head importance scores for one extra epoch. Even though joint pruning methods train  $H$  more parameters during training/fine-tuning,  $H$  is typically orders of magnitudes smaller than the total number of model parameters, so the additional computational overhead is negligible.

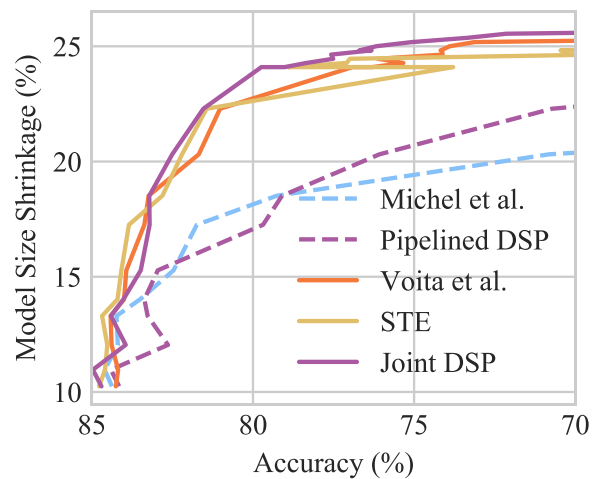
### 5.4 Inference Efficiency

In this section, we obtain the pruned model by actually removing the heads with mask values 0. Empirically, we observe substantial wallclock improvements in our pruned models compared to unpruned models. In practice, we found that the inference efficiency improves monotonically as the number of unpruned heads decrease and is not significantly impacted by the distribution of heads across layers. Taking BERT on MNLI-mismatched validation set (batch size of 8) as an example, we randomly sample 10 head masks for



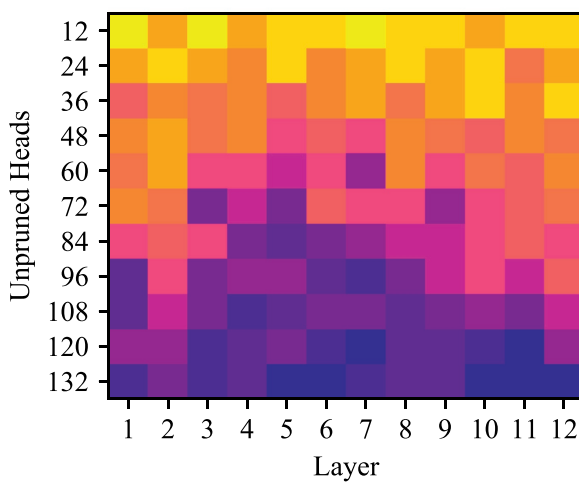


(a) Inference speedup as a function of accuracy.

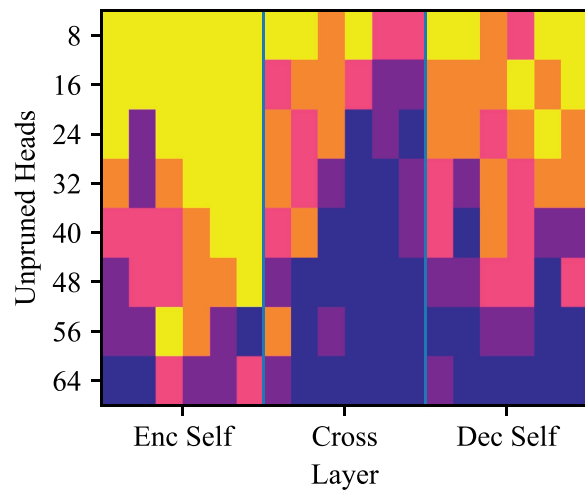


(b) Model size shrinkage as a function of accuracy.

Figure 5: Inference speedup (%) and model size shrinkage (%) of the various pruned BERT models vs. accuracy (%) on the MNLI-mismatched validation set.



(a) BERT



(b) Enc-Dec

Figure 6: Distribution of unpruned heads across layers. Darkness of the color increases monotonically with the number of heads.

each sparsity level, measure their inference speedup and model size shrinkage compared to the unpruned model, and report the average in Figure 4. In general, head pruning does lead to a faster and smaller model, and the more we prune, the faster and smaller the model becomes.

Comparison of various pruning schemes is displayed in Figure 5. If we set a threshold for accuracy (e.g., 80%), joint DSP returns a model with a  $\approx 33\%$  speedup in execution time and  $\approx 24\%$  decrease in model size.

### 5.5 Distribution of Heads

We visualize the distribution of unpruned heads across different layers in Figure 6. For BERT

(Figure 6a), we observe that the top layers (10–12) are the first to be pruned and the heads in the middle layers (3–7) are mostly retained. This observation is in conformity with Prasanna et al. (2020) and Sajjad et al. (2021). Budhraja et al. (2020) also highlight the importance of middle layers but finds no preference between top and bottom layers. For Enc-Dec (Figure 6b), we find that a lot more encoder-decoder cross attention heads are retained compared to the other two types of attentions (encoder and decoder self attentions). The encoder self-attention heads are completely pruned away when less than 16 heads are left, which again conforms with the observations of Michel et al. (2019) and Voita et al. (2019).

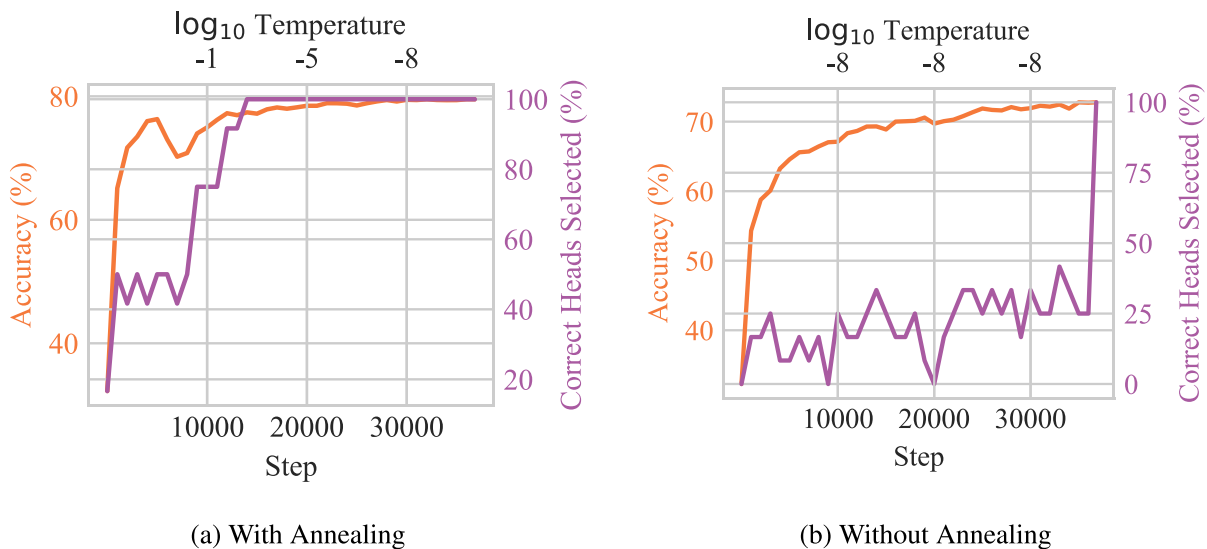


Figure 7: Training dynamics of joint DSP on BERT ( $K = 12$ ). The lower  $x$ -axis shows the number of training steps, and the upper  $x$ -axis shows the corresponding temperature in logarithm scale. Left  $y$ -axis (orange) shows test accuracy on MNLI-mismatched validation set. Right  $y$ -axis (purple) shows the percentage of heads selected at current step that are kept eventually.

Methods	Computation Overhead	Sparsity Controllability	Test Performance
Michel et al.	👎	👍	👎
Pipelined DSP (this paper)	👎	👍	👎
Voita et al.	👍	👎	👍
STE (this paper)	👍	👍	👍
Joint DSP (this paper)	👍	👍	👍

Table 1: Qualitative comparison of different pruning methods.

## 5.6 Analysis of Training Dynamics

To better understand our joint DSP approach, we inspect its behavior during training. We plot the intermediate accuracy of BERT during training when joint DSP ( $K = 12$ ) is applied in Figure 7a (in orange). We also compute the percentage of heads selected at the current step that are eventually kept in the end (in purple). We observe the selected subset of heads is no longer updated after 14000 training steps (purple line stays at 100%). Therefore, the joint pruning process may be viewed as having two distinct phases—(i) head selection and (ii) fine-tuning. This piques one’s interest as it appears to superficially resemble a reversed pipelined pruning. During head selection, the subset of heads to be kept is determined and the model is adapted to the specified level of sparseness. During fine-tuning, the selected subnetwork is fine-tuned so that the testing accuracy improves steadily. Our experiments indicate that annealing

is essential for training a high-performance pruner: It allows the model to gradually settle down on one particular subset of heads, whereas without annealing the pruner never converges to a fixed set and thereby does not enter the fine-tuning phase. See Figure 7b for a visualization.<sup>6</sup>

## 5.7 Summary

The five pruning methods discussed in this paper are summarized in Table 1. Joint DSP is able to maintain the highest test performance while consuming similar computational resources to Voita et al. and offering fine-grained control over the number of unpruned heads like Michel et al. It is worth noting that STE shares the same benefits of low computational overhead and exact sparsity control as joint DSP, despite being slightly inferior in performance. It also has fewer hyperparameters

<sup>6</sup>We analyze other sparsity levels as well and observe similar behaviors. Two examples are shown in Appendix B.

to tune and hence is easier to implement. Therefore, we believe STE could be favorable when test performance is not that critical.

## 6 Related Work

**Unstructured Pruning.** Neural network pruning has been studied for decades. Early work includes optimal brain damage (LeCun et al., 1990) and optimal brain surgeon (Hassibi et al., 1994), which approximate the loss function of a trained model with a second-order Taylor expansion and remove certain parameters in the network while minimizing impact on loss. Recent years have seen a resurgence in this approach (Molchanov et al., 2017b; Theis et al., 2018; Michel et al., 2019). More recently, magnitude pruning that discards parameters with small absolute values has gained much popularity (Han et al., 2015, 2016; Guo et al., 2016; Zhu and Gupta, 2018). Gordon et al. (2020) apply magnitude pruning to BERT and shows that the model has similar prunability and transferability whether pruned after pre-training or after fine-tuning. Related to magnitude based pruning is movement pruning introduced by Sanh et al. (2020) which considers changes in weights instead of magnitudes for pruning.

**Structured Pruning.** Different from above-mentioned unstructured pruning methods that prune individual parameters, structured pruning methods prune at a higher level, such as convolutional channels, attention heads, or even layers. Structured pruning almost always leads to a decrease in model size and inference cost, while unstructured pruning often results in sparse matrices, which cannot be utilized without dedicated hardware or libraries (Han et al., 2016). Previously, structured pruning had primarily been applied to convolutional neural networks (Wen et al., 2016; Li et al., 2017; Luo et al., 2017; He et al., 2017; Liu et al., 2017; Huang and Wang, 2018), but it has recently been applied to NLP, in the form of layer pruning (Fan et al., 2020; Sajjad et al., 2021) and head pruning (Michel et al., 2019; Voita et al., 2019; McCarley et al., 2021) of Transformer-based models. Apart from compression and speedup, head pruning is also helpful for model analysis; Voita et al. (2019) finds that the heads that survive pruning play consistent and linguistically-interpretable roles. Prasanna et al. (2020) discovered the heads that are pruned last tend to be in the earlier and middle layers.

**Dropout for Pruning.** A variety of regularizers have been used to sparsify neural networks. For example, Han et al. (2015) apply  $L_1$  regularization, and Louizos et al. (2018) apply  $L_0$  regularization. Dropout, as one of the regularization methods, has also been demonstrated to be effective for converting a model to be robust to pruning. It was discovered that dropout encourages sparsity when dropout was proposed (Srivastava et al., 2014). Recently, the assumption that the model trained with dropout tend to be more robust to post-hoc pruning was also explored. LayerDrop (Fan et al., 2020) randomly drops entire layers in Transformer with a fixed dropout rate during training and simply keeps every other layer during inference. Targeted Dropout (Gomez et al., 2019) ranks units in the order of magnitude and only applies dropout to those with small magnitudes and performs magnitude pruning afterwards. Molchanov et al. (2017a) introduce variational dropout, which allows learning a different dropout rate for each unit. Kingma et al. (2015) extend it for pruning by keeping only the units with lower dropout rate for test. Our approach is in the same vein but distinct as we learn importance variables rather than dropout rate and the number of heads to be dropped is specified explicitly, which allows us a control over sparsity.

**Lottery Ticket Hypothesis.** Frankle and Carbin (2019) propose the Lottery Ticket Hypothesis that there exist subnetworks (“winning lottery tickets”) in a over-parameterized model, which can be trained in isolation to reach comparable test performance as the original network in a similar number of iterations. It shows such tickets can be discovered through magnitude pruning. Brix et al. (2020) successfully apply the hypothesis to the Transformer. Prasanna et al. (2020) and Behnke and Heafield (2020) demonstrate head pruning may also be used to select a winning subnetwork.

## 7 Conclusion

We propose differentiable subset pruning, a novel method for sparsifying Transformers. The method allows the user to directly specify the desired sparsity level, and it achieves a better sparsity–accuracy trade-off compared to previous work, leading to a faster and more efficient model after pruning. It demonstrates improvements over existing methods for pruning two different models (BERT and Enc–Dec) on two different tasks

(textual entailment and machine translation), respectively. It can be applied in both pruning paradigms (pipelined and joint pruning). Although we study head pruning in the paper, our approach can be extended to other structured and unstructured pruning scenarios. In future work, it would be interesting to look into such cases.

## Acknowledgments

We would like to thank the action editor Noah Smith and the anonymous reviewers for their helpful comments. MS acknowledges funding by SNF under project #201009.

## References

- Dzmitry Bahdanau, Kyunghyun Cho, and Yoshua Bengio. 2015. Neural machine translation by jointly learning to align and translate. In *3rd International Conference on Learning Representations*.
- Maximiliana Behnke and Kenneth Heafield. 2020. Losing heads in the lottery: Pruning transformer attention in neural machine translation. In *Proceedings of the 2020 Conference on Empirical Methods in Natural Language Processing (EMNLP)*, pages 2664–2674, Online. Association for Computational Linguistics.
- Yoshua Bengio, Nicholas Léonard, and Aaron C. Courville. 2013. Estimating or propagating gradients through stochastic neurons for conditional computation. *CoRR*, abs/1308.3432v1.
- Christopher Brix, Parnia Bahar, and Hermann Ney. 2020. Successfully applying the stabilized lottery ticket hypothesis to the transformer architecture. In *Proceedings of the 58th Annual Meeting of the Association for Computational Linguistics*, pages 3909–3915, Online. Association for Computational Linguistics.
- Tom Brown, Benjamin Mann, Nick Ryder, Melanie Subbiah, Jared D. Kaplan, Prafulla Dhariwal, Arvind Neelakantan, Pranav Shyam, Girish Sastry, Amanda Askell, Sandhini Agarwal, Ariel Herbert-Voss, Gretchen Krueger, Tom Henighan, Rewon Child, Aditya Ramesh, Daniel Ziegler, Jeffrey Wu, Clemens Winter, Chris Hesse, Mark Chen, Eric Sigler, Mateusz Litwin, Scott Gray, Benjamin Chess, Jack Clark, Christopher Berner, Sam McCandlish, Alec Radford, Ilya Sutskever, and Dario Amodei. 2020. Language models are few-shot learners. In *Advances in Neural Information Processing Systems*, volume 33, pages 1877–1901.
- Aakriti Budhraj, Madhura Pande, Preksha Nema, Pratyush Kumar, and Mitesh M. Khapra. 2020. On the weak link between importance and prunability of attention heads. In *Proceedings of the 2020 Conference on Empirical Methods in Natural Language Processing (EMNLP)*, pages 3230–3235, Online. Association for Computational Linguistics.
- Mauro Cettolo, Jan Niehues, Sebastian Stüker, Luisa Bentivogli, and Marcello Federico. 2014. Report on the 11<sup>th</sup> IWSLT evaluation campaign. In *Proceedings of the International Workshop on Spoken Language Translation, Hanoi, Vietnam*, volume 57.
- Kevin Clark, Urvashi Khandelwal, Omer Levy, and Christopher D. Manning. 2019. What does BERT look at? An analysis of BERT’s attention. In *Proceedings of the 2019 ACL Workshop BlackboxNLP: Analyzing and Interpreting Neural Networks for NLP*, pages 276–286.
- Ryan Cotterell and Jason Eisner. 2017. Probabilistic typology: Deep generative models of vowel inventories. In *Proceedings of the 55th Annual Meeting of the Association for Computational Linguistics (Volume 1: Long Papers)*, pages 1182–1192, Vancouver, Canada. Association for Computational Linguistics.
- Jacob Devlin, Ming-Wei Chang, Kenton Lee, and Kristina Toutanova. 2019. BERT: Pre-training of deep bidirectional transformers for language understanding. In *Proceedings of the 2019 Conference of the North American Chapter of the Association for Computational Linguistics: Human Language Technologies, Volume 1 (Long and Short Papers)*, pages 4171–4186, Minneapolis, Minnesota. Association for Computational Linguistics.
- Allyson Ettinger. 2020. What BERT is not: Lessons from a new suite of psycholinguistic diagnostics for language models. *Transactions of the Association for Computational Linguistics*, 8:34–48.

- Angela Fan, Edouard Grave, and Armand Joulin. 2020. Reducing transformer depth on demand with structured dropout. In *8th International Conference on Learning Representations*.
- Jonathan Frankle and Michael Carbin. 2019. The lottery ticket hypothesis: Finding sparse, trainable neural networks. In *7th International Conference on Learning Representations*.
- Yarin Gal and Zoubin Ghahramani. 2016. Dropout as a Bayesian approximation: Representing model uncertainty in deep learning. In *Proceedings of The 33rd International Conference on Machine Learning*, volume 48 of *Proceedings of Machine Learning Research*, pages 1050–1059, New York, New York, USA. PMLR.
- Jennifer Gillenwater, Alex Kulesza, and Ben Taskar. 2012. Discovering diverse and salient threads in document collections. In *Proceedings of the 2012 Joint Conference on Empirical Methods in Natural Language Processing and Computational Natural Language Learning*, pages 710–720, Jeju Island, Korea. Association for Computational Linguistics.
- Yoav Goldberg. 2019. Assessing BERT’s syntactic abilities. *CoRR*, abs/1901.05287v1.
- Aidan N. Gomez, Ivan Zhang, Kevin Swersky, Yarin Gal, and Geoffrey E. Hinton. 2019. Learning sparse networks using targeted dropout. *CoRR*, abs/1905.13678v5.
- Mitchell Gordon, Kevin Duh, and Nicholas Andrews. 2020. Compressing BERT: Studying the effects of weight pruning on transfer learning. In *Proceedings of the 5th Workshop on Representation Learning for NLP*, pages 143–155, Online. Association for Computational Linguistics.
- Emil Julius Gumbel. 1954. Statistical theory of extreme values and some practical applications. *Journal of the Royal Aeronautical Society*, 58(527):792–793.
- Yiwen Guo, Anbang Yao, and Yurong Chen. 2016. Dynamic network surgery for efficient DNNs. In *Advances in Neural Information Processing Systems*, volume 29.
- S. Han, X. Liu, H. Mao, J. Pu, A. Pedram, M. A. Horowitz, and W. J. Dally. 2016. EIE: Efficient inference engine on compressed deep neural network. In *2016 ACM/IEEE 43rd Annual International Symposium on Computer Architecture (ISCA)*, pages 243–254.
- Song Han, Huizi Mao, and William J. Dally. 2016. Deep compression: Compressing deep neural network with pruning, trained quantization and huffman coding. In *4th International Conference on Learning Representations*.
- Song Han, Jeff Pool, John Tran, and William Dally. 2015. Learning both weights and connections for efficient neural network. In *Advances in Neural Information Processing Systems*, volume 28.
- Babak Hassibi, David Stork, and Gregory Wolff. 1994. Optimal brain surgeon: Extensions and performance comparisons. In *Advances in Neural Information Processing Systems*, volume 6.
- Y. He, X. Zhang, and J. Sun. 2017. Channel pruning for accelerating very deep neural networks. In *2017 IEEE International Conference on Computer Vision (ICCV)*, pages 1398–1406.
- Zehao Huang and Naiyan Wang. 2018. Data-driven sparse structure selection for deep neural networks. In *Proceedings of the European Conference on Computer Vision (ECCV)*.
- Eric Jang, Shixiang Gu, and Ben Poole. 2017. Categorical reparameterization with Gumbel-softmax. In *5th International Conference on Learning Representations*.
- Ganesh Jawahar, Benoît Sagot, and Djamé Seddah. 2019. What does BERT learn about the structure of language? In *Proceedings of the 57th Annual Meeting of the Association for Computational Linguistics*, pages 3651–3657, Florence, Italy. Association for Computational Linguistics.
- Durk P. Kingma, Tim Salimans, and Max Welling. 2015. Variational dropout and the local reparameterization trick. In *Advances in Neural Information Processing Systems*, volume 28.
- Philipp Koehn, Hieu Hoang, Alexandra Birch, Chris Callison-Burch, Marcello Federico, Nicola Bertoldi, Brooke Cowan, Wade Shen, Christine Moran, Richard Zens, Chris Dyer, Ondřej Bojar, Alexandra Constantin, and Evan

- Herbst. 2007. Moses: Open source toolkit for statistical machine translation. In *Proceedings of the 45th Annual Meeting of the Association for Computational Linguistics Companion Volume Proceedings of the Demo and Poster Sessions*, pages 177–180, Prague, Czech Republic. Association for Computational Linguistics.
- Wouter Kool, Herke Van Hoof, and Max Welling. 2019. Stochastic beams and where to find them: The Gumbel-top- $k$  trick for sampling sequences without replacement. In *Proceedings of the 36th International Conference on Machine Learning*, volume 97 of *Proceedings of Machine Learning Research*, pages 3499–3508. PMLR.
- Yann LeCun, John Denker, and Sara Solla. 1990. Optimal brain damage. In *Advances in Neural Information Processing Systems*, volume 2.
- Hao Li, Asim Kadav, Igor Durdanovic, Hanan Samet, and Hans Peter Graf. 2017. Pruning filters for efficient convnets. In *5th International Conference on Learning Representations*.
- Zhuang Liu, Jianguo Li, Zhiqiang Shen, Gao Huang, Shoumeng Yan, and Changshui Zhang. 2017. Learning efficient convolutional networks through network slimming. In *Proceedings of the IEEE International Conference on Computer Vision*, pages 2736–2744.
- Christos Louizos, Max Welling, and Diederik P. Kingma. 2018. Learning sparse neural networks through  $L_0$  regularization. In *6th International Conference on Learning Representations*.
- Jian-Hao Luo, Jianxin Wu, and Weiyao Lin. 2017. Thinet: A filter level pruning method for deep neural network compression. In *Proceedings of the IEEE International Conference on Computer Vision (ICCV)*.
- Chris J. Maddison, Andriy Mnih, and Yee Whye Teh. 2017. The concrete distribution: A continuous relaxation of discrete random variables. In *5th International Conference on Learning Representations*.
- Chris J. Maddison, Daniel Tarlow, and Tom Minka. 2014.  $A^*$  sampling. In *Advances in Neural Information Processing Systems*, volume 27.
- J. S. McCarley, Rishav Chakravarti, and Avirup Sil. 2021. Structured pruning of a BERT-based question answering model. *CoRR*, abs/1910.06360v3.
- Paul Michel, Omer Levy, and Graham Neubig. 2019. Are sixteen heads really better than one? In *Advances in Neural Information Processing Systems*, volume 32.
- Dmitry Molchanov, Arsenii Ashukha, and Dmitry Vetrov. 2017a. Variational dropout sparsifies deep neural networks. In *Proceedings of the 34th International Conference on Machine Learning*, volume 70 of *Proceedings of Machine Learning Research*, pages 2498–2507, PMLR.
- Pavlo Molchanov, Stephen Tyree, Tero Karras, Timo Aila, and Jan Kautz. 2017b. Pruning convolutional neural networks for resource efficient inference. In *5th International Conference on Learning Representations*.
- Nathan Ng, Kyra Yee, Alexei Baevski, Myle Ott, Michael Auli, and Sergey Edunov. 2019. Facebook FAIR’s WMT19 news translation task submission. In *Proceedings of the Fourth Conference on Machine Translation (Volume 2: Shared Task Papers, Day 1)*, pages 314–319, Florence, Italy. Association for Computational Linguistics.
- Myle Ott, Sergey Edunov, Alexei Baevski, Angela Fan, Sam Gross, Nathan Ng, David Grangier, and Michael Auli. 2019. fairseq: A fast, extensible toolkit for sequence modeling. In *Proceedings of the 2019 Conference of the North American Chapter of the Association for Computational Linguistics (Demonstrations)*, pages 48–53, Minneapolis, Minnesota. Association for Computational Linguistics.
- Tobias Plötz and Stefan Roth. 2018. Neural nearest neighbors networks. In *Advances in Neural Information Processing Systems*, volume 31.
- Sai Prasanna, Anna Rogers, and Anna Rumshisky. 2020. When BERT plays the lottery, all tickets are winning. In *Proceedings of the 2020 Conference on Empirical Methods in Natural Language Processing (EMNLP)*, pages 3208–3229, Online. Association for Computational Linguistics.
- Alec Radford, Jeffrey Wu, Rewon Child, David Luan, Dario Amodei, and Ilya Sutskever. 2019.

- Language models are unsupervised multitask learners.
- Hassan Sajjad, Fahim Dalvi, Nadir Durrani, and Preslav Nakov. 2021. On the effect of dropping layers of pre-trained transformer models. *CoRR*, abs/2004.03844v2.
- Victor Sanh, Thomas Wolf, and Alexander Rush. 2020. Movement pruning: Adaptive sparsity by fine-tuning. In *Advances in Neural Information Processing Systems*, volume 33, pages 20378–20389.
- Nitish Srivastava, Geoffrey Hinton, Alex Krizhevsky, Ilya Sutskever, and Ruslan Salakhutdinov. 2014. Dropout: A simple way to prevent neural networks from overfitting. *Journal of Machine Learning Research*, 15:1929–1958.
- Lucas Theis, Iryna Korshunova, Alykhan Tejani, and Ferenc Huszár. 2018. Faster gaze prediction with dense networks and Fisher pruning. *CoRR*, abs/1801.05787v2.
- George Tucker, Andriy Mnih, Chris J Maddison, John Lawson, and Jascha Sohl-Dickstein. 2017. REBAR: Low-variance, unbiased gradient estimates for discrete latent variable models. In *Advances in Neural Information Processing Systems*, volume 30.
- Ashish Vaswani, Noam Shazeer, Niki Parmar, Jakob Uszkoreit, Llion Jones, Aidan N. Gomez, Łukasz Kaiser, and Illia Polosukhin. 2017. Attention is all you need. In *Advances in Neural Information Processing Systems*, volume 30.
- Tim Vieira. 2014. Gumbel-max trick and weighted reservoir sampling.
- Tim Vieira. 2021a. On the distribution function of order statistics.
- Tim Vieira. 2021b. On the distribution of the smallest indices.
- Jeffrey S. Vitter. 1985. Random sampling with a reservoir. *ACM Transactions on Mathematical Software*, 11(1):37–57.
- Elena Voita, David Talbot, Fedor Moiseev, Rico Sennrich, and Ivan Titov. 2019. Analyzing multi-head self-attention: Specialized heads do the heavy lifting, the rest can be pruned. In *Proceedings of the 57th Annual Meeting of the Association for Computational Linguistics*, pages 5797–5808, Florence, Italy. Association for Computational Linguistics.
- Wei Wen, Chunpeng Wu, Yandan Wang, Yiran Chen, and Hai Li. 2016. Learning structured sparsity in deep neural networks. In *Advances in Neural Information Processing Systems*, volume 29.
- Adina Williams, Nikita Nangia, and Samuel Bowman. 2018. A broad-coverage challenge corpus for sentence understanding through inference. In *Proceedings of the 2018 Conference of the North American Chapter of the Association for Computational Linguistics: Human Language Technologies, Volume 1 (Long Papers)*, pages 1112–1122. Association for Computational Linguistics.
- Thomas Wolf, Lysandre Debut, Victor Sanh, Julien Chaumond, Clement Delangue, Anthony Moi, Pierric Cistac, Tim Rault, Rémi Louf, Morgan Funtowicz, Joe Davison, Sam Shleifer, Patrick von Platen, Clara Ma, Yacine Jernite, Julien Plu, Canwen Xu, Teven Le Scao, Sylvain Gugger, Mariama Drame, Quentin Lhoest, and Alexander M. Rush. 2020. Transformers: State-of-the-art natural language processing. In *Proceedings of the 2020 Conference on Empirical Methods in Natural Language Processing: System Demonstrations*, pages 38–45, Online. Association for Computational Linguistics.
- Sang Michael Xie and Stefano Ermon. 2019. Reparameterizable subset sampling via continuous relaxations. In *International Joint Conference on Artificial Intelligence*.
- Zhilin Yang, Zihang Dai, Yiming Yang, Jaime Carbonell, Ruslan Salakhutdinov, and Quoc V. Le. 2019. XLNet: Generalized autoregressive pretraining for language understanding. In *Advances in Neural Information Processing Systems*, volume 32.
- John I. Yellott. 1977. The relationship between Luce’s Choice Axiom, Thurstone’s Theory of Comparative Judgment, and the double exponential distribution. *Journal of Mathematical Psychology*, 15(2):109–144.

Junru Zhou and Hai Zhao. 2019. Head-Driven Phrase Structure Grammar parsing on Penn Treebank. In *Proceedings of the 57th Annual Meeting of the Association for Computational Linguistics*, pages 2396–2408, Florence, Italy. Association for Computational Linguistics.

Michael Zhu and Suyog Gupta. 2018. To prune, or not to prune: Exploring the efficacy of pruning for model compression. In *6th International Conference on Learning Representations*.

## A Experimental Setup

We report the hyperparameters for joint DSP we use in our experiments in Table 2, which are obtained by tuning on the validation set.

## B Analysis of Training Dynamics

We present two more examples where heads are scarce ( $K = 8$ ) or redundant ( $K = 108$ ). In

	BERT	Enc-Dec
$\tau_{\text{ini}}$	1000	0.1
$\tau_{\text{end}}$	$1e - 08$	$1e - 08$
$N_{\text{cooldown}}$	25000	15000
lr for $w_h$	0.5	0.2

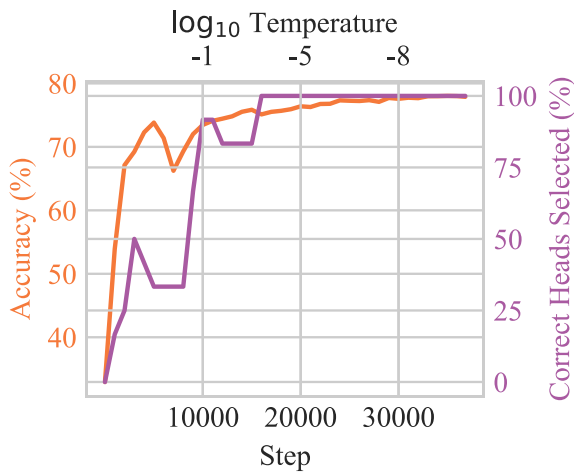
Table 2: Hyperparameters used for joint DSP.

Figure 8a, we observe the same two-phase training behavior as  $K = 12$ . The selected subset of heads is not altered anymore after 16000 steps. In Figure 8c, unlike the cases where there are very few heads, the head masks are constantly updated throughout the training procedure. Yet a large portion (91.7%) of the heads remain unchanged after 17000 steps. Its two-phase behavior is still apparent in comparison with training without annealing (Figure 8d).

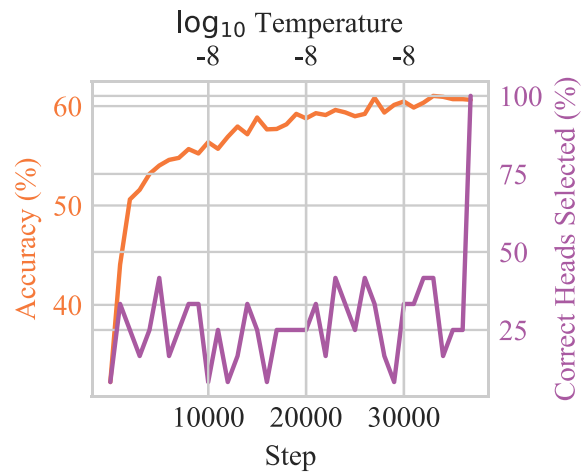
## C Detailed Results

The detailed results for plotting Figure 2 are presented in Table 3.

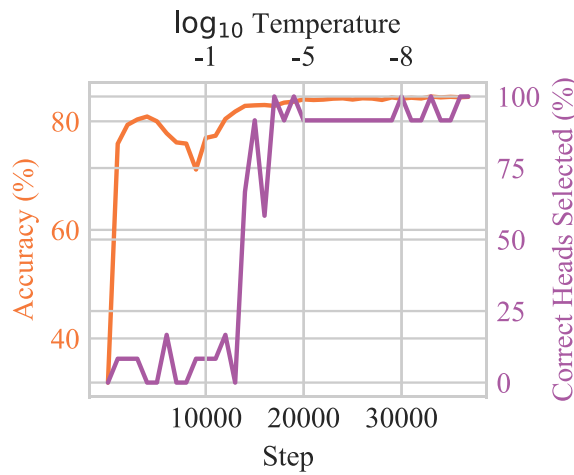




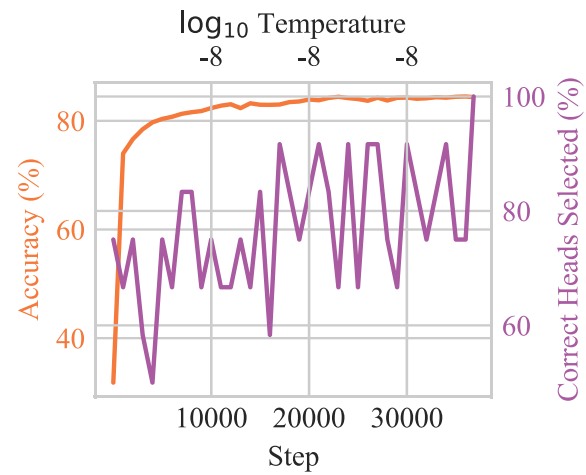
(a)  $K = 8$  with annealing



(b)  $K = 8$  without annealing



(c)  $K = 108$  with annealing



(d)  $K = 108$  without annealing

Figure 8: Training dynamics of joint DSP on BERT. The lower  $x$ -axis shows the number of training steps, and the upper  $x$ -axis shows the corresponding temperature in logarithm scale. Left  $y$ -axis (orange) shows test accuracy on MNLI-mismatched validation set. Right  $y$ -axis (purple) shows the percentage of heads selected at current step that are kept eventually.

Unpruned Heads	Michel et al.	Pipelined DSP	Voita et al.	STE	Joint DSP
132	84.38	84.15	84.26	<b>84.77</b>	84.70
120	84.60	84.41	84.18	84.59	<b>84.97</b>
108	84.19	82.64	84.39	<b>84.52</b>	83.95
96	84.24	83.27	84.42	<b>84.68</b>	84.41
84	83.50	83.37	84.00	<b>84.20</b>	84.02
72	82.47	82.95	83.93	<b>84.08</b>	83.48
60	81.74	79.69	83.37	<b>83.85</b>	83.21
48	79.26	79.10	<b>83.24</b>	82.81	83.22
36	70.82	76.08	81.68	82.20	<b>82.51</b>
24	47.54	70.72	81.02	81.44	<b>81.54</b>
12	40.59	56.29	76.91	73.79	<b>79.74</b>
11	40.16	50.81	76.30	78.91	<b>79.02</b>
10	39.71	49.14	75.34	77.10	<b>78.35</b>
9	40.88	51.20	76.12	76.99	<b>77.51</b>
8	36.16	45.74	74.12	69.29	<b>77.57</b>
7	36.13	43.11	74.14	69.64	<b>76.32</b>
6	34.28	40.90	74.18	70.45	<b>76.70</b>
5	33.24	41.95	73.89	66.53	<b>76.17</b>
4	33.49	42.64	73.12	65.43	<b>75.06</b>
3	32.68	41.79	62.84	65.15	<b>73.36</b>
2	32.74	38.30	62.87	57.07	<b>72.14</b>
1	34.28	43.28	<b>62.09</b>	61.79	61.79

(a) Accuracy on the MNLI-mismatched validation set as a function of number of remaining heads in BERT.

Unpruned Heads	Michel et al.	Pipelined DSP	Voita et al.	STE	Joint DSP
68	32.87	34.19	34.10	<b>34.69</b>	34.52
64	29.08	34.29	34.19	<b>34.55</b>	34.51
60	11.18	32.21	34.14	34.56	<b>34.83</b>
56	6.91	32.52	34.19	34.19	<b>34.46</b>
52	4.41	33.02	34.23	33.92	<b>34.79</b>
48	2.64	31.58	34.20	34.02	<b>34.82</b>
44	2.30	28.70	34.08	33.88	<b>34.68</b>
40	1.70	24.35	34.06	33.85	<b>34.13</b>
36	1.20	25.84	33.82	33.22	<b>34.58</b>
32	0.61	23.94	33.70	32.88	<b>34.10</b>
28	0.19	16.63	33.78	32.01	<b>33.89</b>
24	0.13	20.40	33.44	33.71	<b>33.72</b>
20	0.07	14.11	33.25	31.27	<b>33.54</b>
16	0.07	7.55	<b>32.62</b>	31.25	32.32
12	0.05	3.80	32.33	30.71	<b>32.74</b>
8	0.04	0.63	31.26	28.77	<b>32.68</b>
4	0.04	0.16	29.09	25.45	<b>30.33</b>
3	0.04	0.09	23.08	23.83	<b>28.22</b>
2	0.04	0.05	20.89	22.35	<b>24.18</b>
1	0.04	0.05	20.38	20.37	<b>20.64</b>

(b) BLEU score on IWSLT test set as a function of number of unpruned heads in Enc–Dec.

Table 3: A comparison of various pruning methods.